

# Adsorbed state of benzene on the Si(100) surface: Thermal desorption and electron energy loss spectroscopy studies

Y. Taguchi, M. Fujisawa, T. Takaoka, T. Okada,<sup>a)</sup> and M. Nishijima  
*Department of Chemistry, Faculty of Science, Kyoto University, Kyoto 606, Japan*

(Received 24 June 1991; accepted 22 July 1991)

The adsorbed state of benzene on the Si(100) surface at 90 and 300 K has been investigated by the use of thermal desorption spectroscopy (TDS) and high resolution electron energy loss spectroscopy (EELS). Benzene is chemisorbed nondissociatively on Si(100) at 300 K, and the fractional saturation coverage corresponds to 0.27 benzene molecule per surface Si atom. It is proposed that chemisorbed benzene is *di-σ* bonded to two adjacent Si atoms saturating the dangling bonds on Si(100). At 90 K, physisorbed multilayers of benzene molecules are formed in addition to the chemisorbed layer. The multilayers consist of the metastable transition layer ( $\alpha_2$ ) and "bulk" multilayers ( $\alpha_3$ ). These results are markedly different from those of benzene on the Si(111)(7×7) surface, and the origin of the crystal-face specificity is discussed.

## I. INTRODUCTION

The interaction of benzene with transition metals has been studied by the use of several techniques. In particular, vibrational studies, by using high resolution electron energy loss spectroscopy (EELS), of benzene adsorbed on transition metal surfaces have elucidated the adsorbed state of benzene.<sup>1-3</sup> According to these studies, benzene is chemisorbed molecularly bonding being through  $\pi$  orbitals. On the other hand, only a few works have been reported on the adsorbed state of benzene on semiconductor surfaces.<sup>4-8</sup>

We have studied gas adsorption on the Si surface for several years, and have shown that the surface chemistry on Si is different from that on transition metals in many respects.<sup>9-12</sup> The dangling bonds, in particular, play an important role in the gas adsorption on the Si surface, and a gas molecule tends to form a covalent bond with the dangling bond on the Si surface. Even unsaturated hydrocarbons, e.g., ethylene<sup>9</sup> and acetylene,<sup>10,11</sup> are *di-σ* bonded to two adjacent surface Si atoms saturating the dangling bonds. Nevertheless, we have recently found evidence that indicates that benzene is  $\pi$  bonded to the Si(111)(7×7) surface at low temperature.<sup>8</sup> Benzene is the only gas molecule adsorbed through  $\pi$  orbitals on the Si(111)(7×7) surface to our knowledge.

In the present work, we have studied, by the use of thermal desorption spectroscopy (TDS) and EELS, the adsorbed state of benzene on the Si(100) surface at both 90 and 300 K. Both chemisorbed and physisorbed states of benzene were studied in detail. The results are compared with benzene adsorption on the Si(111)(7×7) surface.

## II. EXPERIMENTAL

The experiments were carried out by the use of an ultra-high vacuum chamber that housed a high-resolution electron spectrometer for EELS, a quadrupole mass spectrometer for TDS, a retarding field analyzer with a

normal-incidence electron gun for low-energy electron diffraction (LEED), and a cylindrical mirror analyzer for Auger electron spectroscopy (AES).

The high-resolution electron spectrometer used for the present study consists of a double-pass 127° cylindrical deflector analyzer (CDA) for the monochromator and a single-pass 127° CDA for the analyzer. For EELS measurements, a primary energy  $E_p$  of 6.5 eV and an incidence angle  $\theta_i$  of 65° with respect to the surface normal were used. An electron was scattered along the [011] azimuth. The full width at half-maximum (FWHM) was typically 8 meV for the clean Si(100) surface. The off-specular measurements were made by rotating the monochromator around an axis that was perpendicular to the incidence plane of the electron beam.

TDS measurements were made by using a quadrupole mass spectrometer whose ionizer was enclosed in a glass envelope with a 2 mm diam aperture.<sup>9</sup> The aperture was located 2 mm from the sample surface. The linear temperature rise (heating rate: 1.5–7 K/s) was performed by using a home-built temperature controller that was programmed by an EPSON PC-286 computer.

The sample used was a Si(100) wafer (*p*-type, boron-doped, 5000  $\Omega$  cm). The Si(100)(2×1) clean surface was carefully prepared by several cycles of Ar<sup>+</sup>-ion bombardment (500 eV, 10–20  $\mu$ A/cm<sup>2</sup>, 30 min) and annealing (1150 K, 2 min).<sup>13</sup> No impurities were observed on the clean surface thus prepared within the detection limit of AES and EELS. Research-grade C<sub>6</sub>H<sub>6</sub> (99.0 mol % purity) and C<sub>6</sub>D<sub>6</sub> (99.6 at. % D, CEA, France) were used. Benzene was purified by freeze–pump–thaw cycles, and was checked for the purity with a mass spectrometer. Benzene was introduced into the vacuum chamber via an 8 mm diam doser located 10 mm from the sample surface. The chamber pressure was monitored by the use of a nude-type Bayard–Alpert ion gauge, and was calibrated by the ion-gauge sensitivity factor of benzene (5.2 relative to N<sub>2</sub>). The ultrahigh vacuum pumping system consisted of a 500 l/s sputter-ion pump, a 2000 l/s titanium cryosublimation pump, and a 160 l/s turbomolecular pump. The base pressure of the vacuum system was  $< 5 \times 10^{-11}$  Torr.

<sup>a)</sup> Present address: Hitachi Research Laboratory, Hitachi Ltd., Hitachi, Ibaraki 319-12, Japan.

### III. RESULTS

#### A. Thermal desorption spectroscopy

TDS measurements after exposing the Si(100) surface to benzene at 90 and 300 K showed that  $C_6H_6$  ( $C_6D_6$ ) was the only desorption product, and other decomposition products, e.g.,  $H_2$ , were not observed. TDS spectra for the Si(100)( $2 \times 1$ ) surface exposed to an increasing amount of  $C_6H_6$  at 300 K are shown in Fig. 1(a). The heating rate was 4 K/s. The observed peaks can be attributed to the desorption from the chemisorbed layer, as will be discussed later. For a small exposure ( $< 0.01$  L), a single desorption peak is observed at 500 K (1 L =  $10^{-6}$  Torr s). With increasing exposure, a new desorption peak appears at 460 K along with the 500 K peak, and for above 1 L exposure, the 460 and 500 K peaks are shifted to 455 and 505 K, respectively. Figures 1(b) and 1(c) show the area intensities of the 460 and 500 K peaks and the total intensity from the measurements such as shown in Fig. 1(a) as a function of the  $C_6H_6$  exposure. These figures indicate that the Si(100)( $2 \times 1$ ) surface is nearly saturated by benzene for  $\sim 2$  L exposure at 300 K and that the intensity of the 500 K peak is nearly one-sixth of the total intensity for  $> 1$  L exposure.

TDS measurements were also made for the physisorbed layer formed as follows: the Si(100) surface was, at first, exposed to 2 L benzene (near saturation exposure) at 300 K,

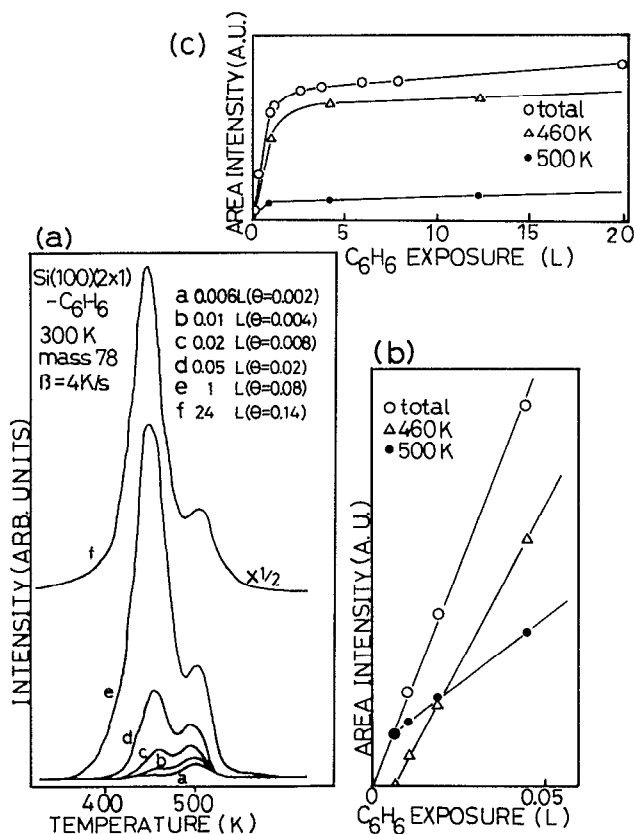


FIG. 1. (a) TDS spectra of  $C_6H_6$  (mass 78) from the Si(100)( $2 \times 1$ ) surface exposed to various amounts of  $C_6H_6$  at 300 K. The heating rate was 4 K/s; (b) and (c) Area intensities of the 460 and 500 K peaks and the total intensity as a function of the  $C_6H_6$  exposure.

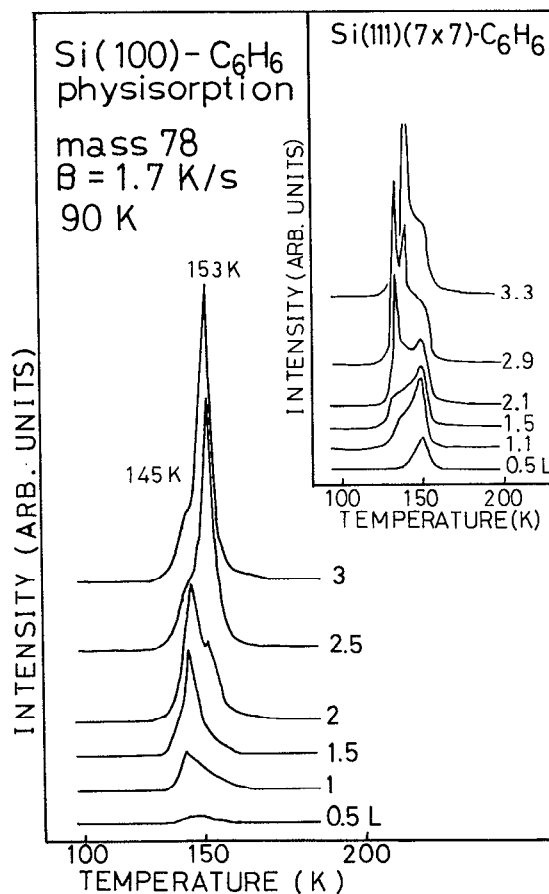


FIG. 2. TDS spectra of  $C_6H_6$  (mass 78) from the  $C_6H_6$ -chemisorbed Si(100) surface exposed to various amounts of  $C_6H_6$  at 90 K. The heating rate was 1.7 K/s. The inset shows TDS spectra for  $C_6H_6$  physisorbed on Si(111)( $7 \times 7$ ).

and was subsequently cooled to 90 K, and then, the benzene-chemisorbed Si(100) surface was exposed to benzene at 90 K. Figure 2 shows the TDS spectra for the physisorbed  $C_6H_6$  with increasing exposure (heating rate: 1.7 K/s). For a small exposure ( $< 2$  L) at 90 K, a single peak is observed at 145 K, and the peak intensity is increased with increasing exposure. For 2 L exposure, a new peak is observed at 153 K along with the 145 K peak. The intensity of the 153 K peak is increased and that of the 145 K peak is decreased with increasing exposure above 2 L. The 153 K peak cannot be saturated and the intensity grows almost linearly with the benzene exposure. The growth of the 153 K peak is accompanied by a common leading-edge character of the zeroth-order desorption,<sup>2</sup> and is attributed to the desorption from the "bulklike" multilayers.

TDS measurements were also carried out for the Si(100)( $4 \times 2$ ) surface exposed to  $C_6H_6$  at 90 K. The desorption peaks were observed at  $< 200$  K along with the 460 and the 500 K peaks. The peaks at  $< 200$  K are attributed to the desorption from the physisorbed layer as discussed above.

The inset of Fig. 2 shows the TDS spectra for  $C_6H_6$  physisorbed on Si(111)( $7 \times 7$ ). Three desorption peaks are observed at 135, 140, and 150 K. The characteristic behavior of these peaks with increasing exposure is similar to that for

benzene multilayers on some transition metals [Ru(0001), etc.],<sup>2,14-17</sup>

### B. Electron energy loss spectroscopy

Figures 3(a) and 3(b) show EELS spectra in the specular and off-specular ( $\Delta\theta = 12^\circ$ ; see the inset of Fig. 3 for the definition of the off-specular angle  $\Delta\theta$ ) modes for the Si(100)(2 $\times$ 1) surface exposed to 2 L C<sub>6</sub>H<sub>6</sub> at 300 K, respectively. Essentially, little change was observed in the vibrational spectra for different exposures except for the intensity variation. Similar spectra were obtained as the Si(100)c(4 $\times$ 2) surface was exposed to C<sub>6</sub>H<sub>6</sub> at 90 K and subsequently heated to 200–300 K. Losses are observed at 615, 790, 910, 1075, 1170, 1635, 2935 and 3065 cm<sup>-1</sup>; the 910 cm<sup>-1</sup> loss was observed only by the off-specular measurement. Angle-dependent measurements were carried out in detail, and the results indicate that, with increasing the off angle  $\Delta\theta$ , only the 615 and 790 cm<sup>-1</sup> losses are reduced in intensity nearly at a similar rate as the elastic-peak intensity. It is, thus, considered that these losses are predominantly excited by the dipole scattering mechanism, and that the other losses by the impact mechanism.<sup>18</sup>

Figures 3(c) and 3(d) show EELS spectra in the specular and off-specular ( $\Delta\theta = 12^\circ$ ) modes for the

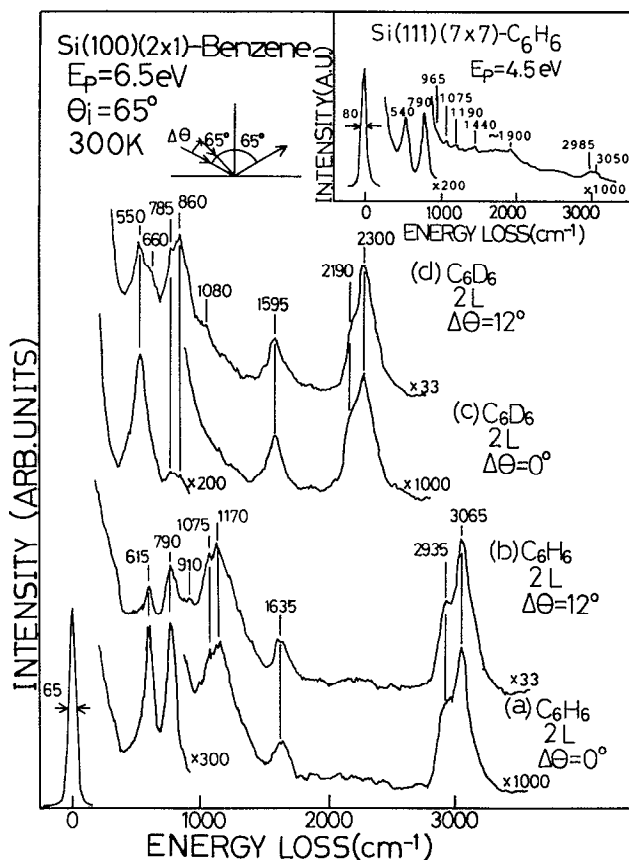


FIG. 3. EELS spectra (a) in the specular mode of Si(100)(2 $\times$ 1) exposed to 2 L C<sub>6</sub>H<sub>6</sub> at 300 K; (b) in the off-specular mode ( $\Delta\theta = 12^\circ$ ); (c) in the specular mode of Si(100)(2 $\times$ 1) exposed to 2 L C<sub>6</sub>D<sub>6</sub>; (d) in the off-specular mode ( $\Delta\theta = 12^\circ$ ). The inset shows an EELS spectrum of C<sub>6</sub>H<sub>6</sub> chemisorbed on Si(111)(7 $\times$ 7) ( $\Delta\theta = 0^\circ$ ). The off-specular angle  $\Delta\theta$  is also shown in the inset.

Si(100)(2 $\times$ 1) surface exposed to 2 L C<sub>6</sub>D<sub>6</sub> at 300 K, respectively. Losses are observed at 550, 660, 785, 860, 1080, 1595, 2190, and 2300 cm<sup>-1</sup>; the 660 and 1080 cm<sup>-1</sup> peaks were observed only by the off-specular measurement. Angle-dependent measurements indicated that the 550 cm<sup>-1</sup> loss was predominantly excited by the dipole mechanism; the other losses by the impact mechanism.

The EELS spectrum for C<sub>6</sub>H<sub>6</sub> chemisorbed on the Si(111)(7 $\times$ 7) surface is shown in the inset of Fig. 3. The spectrum is attributed to the chemisorbed benzene which is  $\pi$  bonded to the Si(111)(7 $\times$ 7) surface.<sup>8</sup>

As the Si(100)(2 $\times$ 1) surface exposed to 2 L C<sub>6</sub>H<sub>6</sub> at 300 K was heated to  $\leq 500$  K, little change was observed in the EELS spectrum, except for the intensity. After 600 K heating, the chemisorbed benzene desorbed completely, and the spectrum for the clean Si(100)(2 $\times$ 1) surface was recovered.

EELS measurements were also carried out in order to investigate the property of the physisorbed layer. The physisorbed layer on Si(100) was prepared similarly to that used for the TDS measurement. Figure 4(a) [4(b)] shows an EELS spectrum in the specular mode for the physisorbed layer formed by the exposure of the C<sub>6</sub>H<sub>6</sub> (C<sub>6</sub>D<sub>6</sub>)-chemisorbed Si(100) surface to 2 L C<sub>6</sub>H<sub>6</sub> (C<sub>6</sub>D<sub>6</sub>) at 90 K. As the C<sub>6</sub>H<sub>6</sub> exposure was changed, little shift of the loss energies was observed. The loss energies of the spectra are very similar to the vibrational energies of gas-, liquid-, or solid-phase C<sub>6</sub>H<sub>6</sub> (C<sub>6</sub>D<sub>6</sub>).<sup>19</sup>

### C. Low-energy electron diffraction and Auger electron spectroscopy

LEED observations for Si(100) exposed to benzene both at 90 and 300 K were carried out. For the

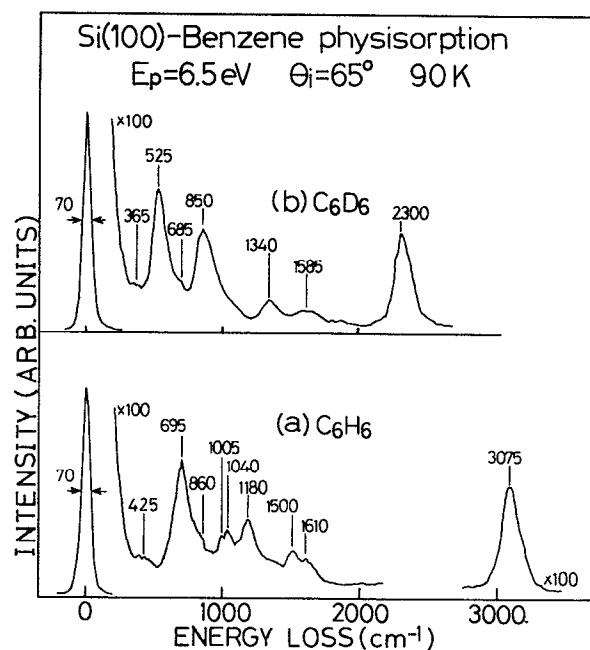


FIG. 4. EELS spectra in the specular mode of (a) the C<sub>6</sub>H<sub>6</sub>-chemisorbed Si(100) surface exposed to 2 L C<sub>6</sub>H<sub>6</sub> at 90 K; (b) the C<sub>6</sub>D<sub>6</sub>-chemisorbed Si(100) surface exposed to 2 L C<sub>6</sub>D<sub>6</sub>.

Si(100) ( $2 \times 1$ ) surface exposed to benzene at 300 K, a sharp ( $2 \times 1$ ) LEED pattern was observed with a slight increase of the background intensity. The chemisorption on Si(100)c( $4 \times 2$ ) induced the c( $4 \times 2$ )  $\rightarrow$  ( $2 \times 1$ ) conversion. These results indicate that the Si-Si dimers on the Si(100) surface are preserved after the benzene chemisorption.

In order to estimate the fractional C coverage  $\theta_c$  (number of C atoms per surface Si atom) corresponding to the total amount of the chemisorbed benzene, AES measurements were made for the  $C_6H_6$ - and  $C_2H_4$ -saturated Si(100)( $2 \times 1$ ) surfaces. The  $\theta_c$  for  $C_2H_4$ -saturated Si(100)( $2 \times 1$ ) is estimated to be  $\sim 0.8$ .<sup>9,20</sup> The Auger-peak-height ratio C(KLL)/Si(LVV) for  $C_6H_6$ -saturated Si(100)( $2 \times 1$ ) was compared with that for  $C_2H_4$ -saturated Si(100)( $2 \times 1$ ). The  $\theta_c$  for  $C_6H_6$ -saturated Si(100)( $2 \times 1$ ) was estimated to be  $\sim 1.6$ , which indicates that the fractional saturation coverage of benzene  $\theta_{C_6H_6}$  on Si(100)( $2 \times 1$ ) is  $\sim 0.27$ .

#### IV. DISCUSSION

##### A. Chemisorbed state of benzene on Si(100)( $2 \times 1$ ) at 300 K

TDS spectra for  $C_6H_6$  chemisorbed on Si(100) show two desorption peaks at 460 and 500 K [Fig. 1(a)], which indicates the existence of two chemisorbed states of benzene. The heats of desorption for the 460 and 500 K peaks are estimated to be 28 and 32 kcal/mole, respectively, using the Redhead formula,<sup>21</sup> assuming a first-order desorption and a preexponential factor of  $10^{13} \text{ s}^{-1}$ .

Area intensities of the desorption peaks from the chemisorbed layer are shown in Figs. 1(b) and 1(c) with increasing  $C_6H_6$  exposure. The figures indicate that benzene associated with the 500 K peak is adsorbed first for a small exposure, and that, with increasing exposure, the amount of benzene associated with the 460 K peak is increased. The area intensity for the 500 K peak is about 17% of the total (460 and 500 K) peak intensity for  $C_6H_6$ -saturated Si(100). It is noted that the Si(100) surface has structural defects whose density is 10%–25%.<sup>22</sup> The desorption peak at 500 K may be, therefore, attributed to the desorption of

benzene chemisorbed on the defect sites of Si(100). The heats of desorption estimated above indicate that the defect sites are thermodynamically more favorable for benzene adsorption than the terrace sites.

Nevertheless, Fig. 1(b) shows that the 460 K peak grows before the 500 K peak is saturated. These results are interpreted to indicate that, due to the low mobility of benzene arriving at the Si(100) surface at 300 K, benzene on the terrace sites coexists with that on the defect sites even at low coverage. Hereafter, benzene chemisorbed on the defect sites will not be discussed, as the corresponding losses were not clearly observable by EELS due, probably, to the low concentration.

##### B. Assignments of the EELS peaks for benzene chemisorbed on Si(100)

Assignments of the EELS peaks shown in Fig. 3 can be made by comparison with the vibrational energies of gas-, liquid-, or solid-phase  $C_6H_6$  ( $C_6D_6$ ),<sup>19</sup> benzene chemisorbed on transition metals<sup>1–3</sup> and semiconductors,<sup>5,6,8</sup> and also by examining the energy ratio  $\nu_H/\nu_D$  for  $C_6H_6$  on Si(100) and the deuterated counterpart.

Assignments of the EELS peaks that are associated with chemisorbed benzene on Si(100)( $2 \times 1$ ) are summarized in Table I, and can be carried out as follows.

The 3065 (2300) and 2935 (2190)  $\text{cm}^{-1}$  peaks can be readily assigned to the CH (CD) stretching vibrations. The 1635 (1595)  $\text{cm}^{-1}$  loss can be ascribed to the CC stretching vibration. The 1170  $\text{cm}^{-1}$  loss observed for  $C_6H_6$  on Si is associated with the 860 and 1080  $\text{cm}^{-1}$  losses for  $C_6D_6$  on Si, which are ascribed to the CD in-plane bending and CC stretching modes, respectively; the assignments are made by examining the energy ratio  $\nu_H/\nu_D$  (1.36 and 1.08, respectively) and by comparison with EELS spectra for benzene chemisorbed on transition metals.<sup>1–3</sup> The 1075 (785) and 910 (660)  $\text{cm}^{-1}$  losses are ascribed to the CH (CD) in-plane-bending modes by examining the energy ratio  $\nu_H/\nu_D$  (1.37 and 1.38, respectively). The 790 and 615  $\text{cm}^{-1}$  losses for  $C_6H_6$  on Si are ascribed to the CH out-of-plane bending and SiC stretching vibrations, respectively. The deuterated

TABLE I. Vibrational energies ( $\text{cm}^{-1}$ ) and their assignments of  $C_6H_6$  ( $C_6D_6$ ) chemisorbed on Si(100)( $2 \times 1$ ) at 300 K along with those on Si(111)( $7 \times 7$ ) (Ref. 8). The energy ratio  $\nu_H/\nu_D$  and the dominant electron scattering mechanism are included.

Energy ( $\text{cm}^{-1}$ )		Benzene chemisorbed on Si(100)( $2 \times 1$ )			On Si(111)( $7 \times 7$ )	
$C_6H_6$	$C_6D_6$	Energy ratio $\nu_H/\nu_D$	Dominant mechanism	Mode	$C_6H_6$	$C_6D_6$
615	550	1.12	Dipole	SiC stretch	540	510
790	550	1.44	Dipole	CH bend	790	630
910	660	1.38	Impact	CH bend		
				CC stretch	965	930
1075	785	1.37	Impact	CH bend	1075	805
1170	860	1.36	Impact	CH bend	1190	930
1170	1080	1.08	Impact	CC stretch		
1635	1595	1.03	Impact	CC stretch	1440	...
2935	2190	1.34	Impact	CH stretch		
3065	2300	1.33	Impact	CH stretch	2985	2195
					3050	2260

counterparts of both peaks are overlapped, and are observed at  $550\text{ cm}^{-1}$ .

It is noted that no peak is observed at  $\sim 2100\text{ cm}^{-1}$  associated with the SiH stretching mode.<sup>23</sup> This indicates that benzene is not dissociated on the Si(100)( $2\times 1$ ) surface.

### C. Structure of benzene chemisorbed on Si(100)

There are noticeable differences in the energies of the CH, CC, and SiC stretching modes between chemisorbed benzene on Si(100) and Si(111)( $7\times 7$ ) (Table I). Thus, the bonding state of chemisorbed benzene on Si(100) seems different from  $\pi$  bonding.

(1) Generally, the CH (CD) stretching energies for the gas-phase hydrocarbons are observed at  $\sim 3300, 3100,$  and  $3000$  ( $\sim 2600, 2300,$  and  $2200$ )  $\text{cm}^{-1}$  for  $sp, sp^2,$  and  $sp^3$  bonding of the carbon atom, respectively.<sup>18,19</sup> The CH stretching mode for benzene  $\pi$  bonded to the transition-metal surfaces is observed above  $\sim 3000\text{ cm}^{-1}$ .<sup>1-3</sup> For benzene which is  $\pi$  bonded to Si(111)( $7\times 7$ ), the CH (CD) stretching modes are observed at 2985 (2195) and 3050 (2260)  $\text{cm}^{-1}$ .<sup>8</sup> The CH stretching modes of chemisorbed benzene on Si(100) are observed (more separately) at 2935 (2190) and 3065 (2300)  $\text{cm}^{-1}$ . From the above general rule, the 2935 (2190)  $\text{cm}^{-1}$  loss is ascribed to  $\sim sp^3$  bonding and the 3065 (2300)  $\text{cm}^{-1}$  loss to  $\sim sp^2$  bonding. One might attribute the relatively low energy [2935 (2190)  $\text{cm}^{-1}$ ] of the CH stretching mode to the hydrogen-bonding interaction. In this case, the CH stretching mode is expected to be observed at  $2600\text{--}2800\text{ cm}^{-1}$  accompanied with the broadening.<sup>18</sup> However, this possibility can be excluded, as the broadening is not observed.

(2) Typical CC stretching energies are  $\sim 950, 1600,$  and  $2100\text{ cm}^{-1}$  for CC single, double, and triple bonds, respectively.<sup>18,19</sup> Thus, the 1635 (1595)  $\text{cm}^{-1}$  loss is attributed to

the CC double bond and the  $1170$  ( $1080$ )  $\text{cm}^{-1}$  loss to the CC single bond. The CC stretching modes of the  $\pi$ -bonded benzene are observed at  $840\text{--}1000, 1410\text{--}1480,$  and  $1580\text{ cm}^{-1}$  for transition metals,<sup>1-3</sup> and at  $965$  and  $1440\text{ cm}^{-1}$  for Si(111)( $7\times 7$ ).

(3) The (symmetric<sup>9-11</sup>) SiC stretching mode for Si(100) is observed at an energy much higher than the SiC stretching mode for Si(111)( $7\times 7$ ).

Information for the chemisorbed state of benzene on Si(100) obtained by the TDS, EELS, LEED, and AES measurements is summarized as follows: (1) Benzene is adsorbed nondissociatively on Si(100); (2) chemisorbed benzene has C atoms which are rehybridized to have a  $\sim sp^3$  hybridization state; (3) the saturation coverage of benzene ( $\theta_{\text{C}_6\text{H}_6} \sim 0.27$ ) indicates that nearly one benzene molecule corresponds to two Si-Si dimers; and (4) the Si-Si dimers on Si(100) are preserved after the benzene chemisorption.

Angle-dependent EELS measurements for  $\text{C}_6\text{H}_6$ -chemisorbed Si(100)( $2\times 1$ ) show that losses associated with the CH stretching modes have little component excited by the dipole mechanism. Therefore, we did not make an examination of the ratio of the intensity of the CH out-of-plane bending mode and that of the CH stretching mode. The loss energies of the CH out-of-plane bending mode were observed at  $675\text{--}910\text{ cm}^{-1}$  for  $\pi$ -bonded benzene on some transition-metal surfaces, and it is well known that the vibration energy of the CH out-of-plane bending mode of the adsorbed benzene is very sensitive to the deformation of the carbon ring that is induced by the adsorption.<sup>1-3</sup> Thus, it is difficult to determine the adsorbed structure by using the vibrational energy of the CH out-of-plane bending mode.

The results obtained by the present experiments are interpreted to indicate that chemisorbed benzene is *di- $\sigma$*  bonded to the Si(100) surface, and the structural models are shown in Fig. 5. As benzene is *di- $\sigma$*  bonded to the Si-Si dimer

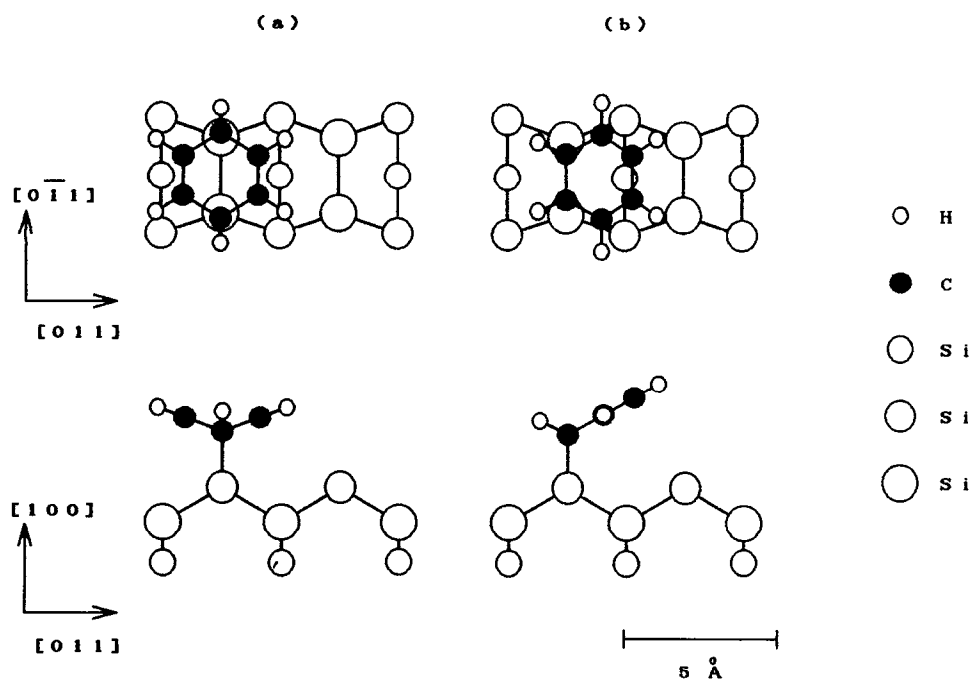


FIG. 5. Structural models of benzene chemisorbed on Si(100): (a) the CC double bonds are between carbon atoms 1 and 2 and between 4 and 5; (b) between carbon atoms 1 and 2 and between 3 and 4.

TABLE II. Vibrational energies ( $\text{cm}^{-1}$ ) and their assignments of  $\text{C}_6\text{H}_6$  ( $\text{C}_6\text{D}_6$ ) physisorbed on Si(100) and Si(111)( $7\times 7$ ) (Ref. 8) at 90 K together with those of gas-, liquid-, or solid-phase  $\text{C}_6\text{H}_6$  ( $\text{C}_6\text{D}_6$ ) (Ref. 19). The mode number and surface subgroup of  $D_{6h}$  symmetry are included.

Physisorbed benzene				Gas-, liquid-, or solid-phase benzene			
Si(100)		Si(111)( $7\times 7$ )					
$\text{C}_6\text{H}_6$	$\text{C}_6\text{D}_6$	$\text{C}_6\text{H}_6$	$\text{C}_6\text{D}_6$	$\text{C}_6\text{H}_6$	$\text{C}_6\text{D}_6$	mode no. and representation	
425	365	420	365	410	352	$\nu_{20}$	( $E_{2u}$ )
695	525	695	520	673	497	$\nu_4$	( $A_{2u}$ )
860	685	865	670	849	662	$\nu_{11}$	( $E_{1g}$ )
1005	850	1010	840	995	827	$\nu_7$	( $B_{2g}$ )
1040	850	1040	840	1038	814	$\nu_{14}$	( $E_{1u}$ )
1180	850	1180	840	1150	824	$\nu_{10}$	( $B_{2u}$ )
				1178	867	$\nu_{17}$	( $E_{2g}$ )
		1355	...	1326	1037	$\nu_3$	( $A_{2g}$ )
1500	1340	1490	1345	1486	1335	$\nu_{13}$	( $E_{1u}$ )
1610	1585	1620	1580	1596	1552	$\nu_{16}$	( $E_{2g}$ )
3075	2300	3070	2295	3047	2265	$\nu_{15}$	( $E_{2g}$ )
				3062	2293	$\nu_1$	( $A_{1g}$ )
				3063	2287	$\nu_{12}$	( $E_{1u}$ )
				3068	2292	$\nu_5$	( $B_{1u}$ )

on Si(100), six CC bonds of the carbon ring are not equivalent, and four CC single bonds and two CC double bonds are made. These two CC double bonds can be between carbon atoms 1 and 2 and between 4 and 5 [Fig. 5(a)] or between carbon atoms 1 and 2 and between 3 and 4 [Fig. 5(b)]. These structures correspond to 1,4- and 1,3-cyclohexadiene, respectively. In Fig. 5, we have assumed that the Si-C bond length is  $1.85 \text{ \AA}$ ,<sup>24</sup> and the Si-Si distance of the (symmetric) Si-Si dimer is  $\sim 2.5 \text{ \AA}$ .<sup>25,26</sup> We have also assumed, in Fig. 5, that the benzene molecule is bonded to a Si-Si dimer, however, benzene can also be located between two dimers. We can not uniquely determine the best model by the present study.

#### D. Physisorbed benzene on Si(100)

The loss energies of physisorbed benzene (Fig. 4) are very similar to those of gas-, liquid-, or solid-phase  $\text{C}_6\text{H}_6$  ( $\text{C}_6\text{D}_6$ ), and also are similar to those for physisorbed benzene on Si(111)( $7\times 7$ ).<sup>8</sup> Their proposed assignments are summarized in Table II together with the vibrational energies of benzene physisorbed on Si(111)( $7\times 7$ ) and those of free benzene. The numbering system of Herzberg<sup>27</sup> is used in the table.

The behavior of the desorption peaks for benzene physisorbed on Si(100) (Fig. 2) is similar to that on some transition-metal surfaces [Ni(111),<sup>14</sup> Ni(100),<sup>15</sup> Mo(110),<sup>16</sup> and Ru(0001)<sup>2,17</sup>], except for the disappearance of the desorption peak at the highest temperature ( $\alpha_1$ ) (which will be discussed in Sec. IV E). Following the labels used by Polta and Thiel,<sup>17</sup> the two desorption peaks in Fig. 2 are associated with the  $\alpha_2$  (low-temperature peak) and  $\alpha_3$  (high-temperature peak) layers. According to Jakob and Menzel,<sup>2</sup> the  $\alpha_2$  layer is a metastable transition layer and the  $\alpha_3$  layer is "bulk" multilayers; benzene molecules in the  $\alpha_2$  layer has a high mean tilt angle.

When benzene molecules are adsorbed on the  $\alpha_2$  layer,

the bulklike  $\alpha_3$  layer is formed on the  $\alpha_2$  layer. The  $\alpha_3$  layer disturbs the desorption from the underlying  $\alpha_2$  layer; a part of the  $\alpha_2$  layer is converted into the  $\alpha_3$  layer upon adsorption or during heating for TDS measurements.<sup>2</sup> Therefore, the  $\alpha_2$  peak intensity is decreased with increasing exposure above 2 L, as shown in Fig. 2.

#### E. Comparison of benzene on Si(100) and Si(111)( $7\times 7$ )

Chemisorbed benzene is  $\pi$  bonded to the Si(111)( $7\times 7$ ) surface<sup>8</sup> and is  $\sigma$  bonded to the Si(100) surface, as discussed in Sec. IV C. This is, to our knowledge, the first clean observation of the crystal-face specificity of chemical bonding of a gas molecule on Si. It is difficult to explain why the difference of the bonding property occurs for the benzene adsorption. It is noted that benzene molecule is much larger than the gases which have been studied previously. The face specificity is probably caused by the difference of distance between the dangling bonds. On the Si(111)( $7\times 7$ ) surface, the dangling bonds that can be  $di-\sigma$  bonded to benzene are located at the neighboring rest atom and adatom according to the DAS (dimer-adatom-stacking fault) model.<sup>28</sup> However, benzene cannot be  $di-\sigma$  bonded to the neighboring rest atom and adatom because of the steric hindrance. The distance between two neighboring rest atoms or between two adatoms is too large for the  $di-\sigma$  bonding. It is noted that theoretical studies on the interaction between acetylene and the Si surface have been made by a few research groups.<sup>29,30</sup> Weiner *et al.*<sup>30</sup> suggested that a significant restructuring of the Si surface took place for  $\text{C}_2\text{H}_2$ -adsorbed Si(111). To our knowledge, the interaction of benzene with Si has not been studied theoretically yet.

The difference of the physisorbed state of benzene is also observed between Si(100) and Si(111)( $7\times 7$ ) in the TDS measurements, as shown in Fig. 2. The  $\alpha_1$  layer is formed on the Si(111)( $7\times 7$ ) surface as on some transition-metal surfaces.<sup>2,8,14-17</sup> It is noted that the  $\alpha_1$  layer is the first physi-

sorbed layer on top of the chemisorbed layer and is oriented parallel to the surface; the corresponding desorption peak is observed at the highest temperature.<sup>2</sup> The stronger bonding of benzene in the  $\alpha_1$  layer is considered to be caused by the electrostatic interaction with the polarized chemisorbed benzene which is  $\pi$  bonded to the substrate. Thus, the disappearance of the  $\alpha_1$  layer on Si(100) may be caused by the small polarization of chemisorbed benzene which is  $\sigma$  bonded to the substrate.

## V. SUMMARY

A combined TDS, EELS, LEED, and AES study has been carried out on the interaction of benzene with the Si(100) surface. Some of the important results are as follows.

(1) Benzene is chemisorbed nondissociatively on the Si(100) surface both at 90 and 300 K. The chemisorbed benzene has carbon atoms that are rehybridized to have a near  $sp^3$  hybridization state. It is proposed that benzene is *di-* $\sigma$  bonded to two adjacent Si atoms on Si(100). Models for the chemisorbed benzene are shown in Fig. 5.

(2) As the Si(100) surface is exposed to benzene at 90 K, physisorbed benzene is formed on the chemisorbed benzene layer. The physisorbed benzene consists of the  $\alpha_2$  and  $\alpha_3$  layers. By comparison with physisorbed benzene on transition-metal surfaces, the  $\alpha_2$  layer is identified as a metastable transition layer and the  $\alpha_3$  layer as "bulk" multilayers.

(3) Marked differences were observed in the adsorbed states of chemisorbed and physisorbed benzene on Si(100) and Si(111) ( $7 \times 7$ ), and the reasons are discussed in Sec. IV E.

## ACKNOWLEDGMENTS

This work was supported in part by Grants-in-Aid for Scientific Research from the Ministry of Education, Science and Culture, and from the Hōsō-Bunka Foundation.

<sup>1</sup>N. Sheppard, *Annu. Rev. Phys. Chem.* **39**, 589 (1988).

<sup>2</sup>P. Jakob and D. Menzel, *Surf. Sci.* **220**, 70 (1989).

<sup>3</sup>M. Fujisawa, T. Sekitani, Y. Morikawa, and M. Nishijima, *J. Phys. Chem.* (in press).

<sup>4</sup>M. N. Piancastelli, F. Cerrina, G. Margaritondo, A. Franciosi, and J. H. Weaver, *Appl. Phys. Lett.* **42**, 990 (1983).

<sup>5</sup>M. N. Piancastelli, G. Margaritondo, J. Anderson, D. J. Frankel, and G. J. Lapeyre, *Phys. Rev. B* **30**, 1945 (1984).

<sup>6</sup>M. N. Piancastelli, M. K. Kelly, G. Margaritondo, D. J. Frankel, and G. J. Lapeyre, *Phys. Rev. B* **34**, 2511 (1986).

<sup>7</sup>M. N. Piancastelli, M. K. Kelly, Y. Chang, J. T. McKinley, and G. Margaritondo, *Phys. Rev. B* **35**, 9218 (1987).

<sup>8</sup>Y. Taguchi, M. Fujisawa, and M. Nishijima, *Chem. Phys. Lett.* **178**, 363 (1991).

<sup>9</sup>J. Yoshinobu, H. Tsuda, M. Onchi, and M. Nishijima, *Solid State Commun.* **60**, 801 (1986); *J. Chem. Phys.* **87**, 7332 (1987).

<sup>10</sup>J. Yoshinobu, H. Tsuda, M. Onchi, and M. Nishijima, *Chem. Phys. Lett.* **130**, 170 (1986).

<sup>11</sup>M. Nishijima, J. Yoshinobu, H. Tsuda, and M. Onchi, *Surf. Sci.* **192**, 383 (1987).

<sup>12</sup>S. Tanaka, M. Onchi, and M. Nishijima, *Chem. Phys. Lett.* **146**, 67 (1988); *J. Chem. Phys.* **91**, 2712 (1989).

<sup>13</sup>Y. Taguchi, M. Fujisawa, and M. Nishijima, *Surf. Sci. Lett.* **233**, L251 (1990).

<sup>14</sup>H.-P. Steinrück, W. Huber, T. Pache, and D. Menzel, *Surf. Sci.* **218**, 293 (1989).

<sup>15</sup>P. M. Blass, S. Akhter, and J. M. White, *Surf. Sci.* **191**, 406 (1987).

<sup>16</sup>A. C. Liu and C. M. Friend, *J. Chem. Phys.* **89**, 4396 (1988).

<sup>17</sup>J. A. Polta and P. A. Thiel, *J. Am. Chem. Soc.* **108**, 7560 (1986).

<sup>18</sup>H. Ibach and D. L. Mills, *Electron Energy Loss Spectroscopy and Surface Vibrations* (Academic, New York, 1982).

<sup>19</sup>T. Shimanouchi, *Tables of Molecular Vibrational Frequencies*, Vol. 1, Natl. Stand. Ref. Data Ser. Natl. Bur. Stand. **39** (U.S. GPO, Washington, DC, 1972).

<sup>20</sup>C. C. Cheng, R. M. Wallace, P. A. Taylor, W. J. Choyke, and J. T. Yates, Jr., *J. Appl. Phys.* **67**, 3693 (1990).

<sup>21</sup>P. A. Redhead, *Vacuum*, **12**, 203 (1962).

<sup>22</sup>R. J. Hamers, R. M. Tromp, and J. E. Demuth, *Phys. Rev. B* **34**, 5343 (1986).

<sup>23</sup>H. Kobayashi, K. Edamoto, M. Onchi, and M. Nishijima, *J. Chem. Phys.* **78**, 7429 (1983).

<sup>24</sup>J. E. Huheey, *Inorganic Chemistry*, 3rd ed. (Harper and Row, New York, 1983).

<sup>25</sup>D. J. Chadi, *Phys. Rev. Lett.* **43**, 43 (1979).

<sup>26</sup>Y. J. Chabal and K. Raghavachari, *Phys. Rev. Lett.* **53**, 282 (1984).

<sup>27</sup>G. Herzberg, *Infrared and Raman Spectrum of Polyatomic Molecules* (Van Nostrand, New York, 1945).

<sup>28</sup>K. Takayanagi, Y. Tanishiro, S. Takahashi, and M. Takahashi, *Surf. Sci.* **164**, 367 (1985).

<sup>29</sup>S.-Y. Chu and A. B. Anderson, *Surf. Sci.* **194**, 55 (1988).

<sup>30</sup>B. Weiner, C. S. Carmer, and M. Frenklach, *Phys. Rev. B* **43**, 1678 (1991).